Pergamon

PII: S0277-5387(97)00157-5

Polyhedron Vol. 16, No. 23, pp. 4121–4128, 1997

0277-5387/97 $17.00+0.00

Synthesis, structure and characterization of heterometal VFe_3S_4 cubane-like cluster compound $(Et_4N)[VFe_3S_4(Et_2dtc)_4]$

Yuheng Deng, Qiutian Liu,* Changneng Chen, Youtong Wang, Yuanba Cai, Daxu Wu, Beisheng Kang,† Daizheng Liao‡ and Jianzhong Cui‡

State Key Laboratory of Structural Chemistry, Fujian Institute of Research on the Structure of Matter, Chinese Academy of Sciences, Fuzhou, Fujian 350002, P.R. China and State Key Laboratory of Elemento-Organic Chemistry, Nankai University, Tianjin 300071, P.R. China

(Received 4 February 1997; accepted 17 April 1997)

Abstract—A cubane-type cluster $(Et_4N)[VFe_3S_4(Et_2dtc)_4]$ has been synthesized from a self-assembly reaction system $VS_4^{3-}/FeCl_2/Et_2dtc^-/PhS^-$ in acetonitrile (Et_2dtc^- = diethyldithiocarbamate). The compound has been structurally characterized by X-ray crystallography. Mössbauer and structural parameters have been used to deduce the oxidation states of the metal atoms in $[VFe_3S_4]^{3+}$ core indicating that there are three Fe atoms with mean oxidation state of *ca* +2.8. Proton NMR spectrum indicates the paramagneticity of the cluster. The chemical shift of ^{51}V NMR was observed at −210 ppm. Variable-temperature magnetic susceptibility measurement reveals an antiferromagnetic interaction in the VFe_3 coupling system. © 1997 Elsevier Science Ltd

Keywords: vanadium complex; iron complex; heterometallic complex; structure; magnetism.

The studies on iron-containing heterometal sulfur cubane-type compounds have been attractive to bioinorganic chemists for simulating the active center of nitrogenases [1]. Numbers of suitable model clusters have been documented at some length [1a,2]. The recent X-ray diffraction of MoFe-protein has led to a supposition of Kim–Rees model [3], which consists of two defective cuboidal units, Fe_4S_3 and $MoFe_3S_3$, linked by three sulfur atoms. The solution of the structure of FeMo-cofactor in nitrogenase confirms the necessity of the foregoing studies on M/Fe/S (M = Mo [1a,2], V[4]) double- or single-cubane clusters. We have been studying on self-assembly reaction system of $MS_4^{m-}/M'^{n+}/R_2dtc^-$ (and/or RS^-) (M = Mo, W, V; M′ = Fe, Cu, Ag) for the syntheses of heterometallic sulfur cubane clusters with R_2dtc ligand. A series of Mo(W)/Fe/S/R_2dtc [5], Mo(W)/Cu/S/R_2dtc [6] and V/Cu(Ag)/S/R_2dtc [7] cubane-like clusters have been synthesized from the systems and have made a heterometallic sulfur cluster family containing R_2dtc^- ligand. However, the V/Fe/S/R_2dtc cluster compound has not yet been reported except of the only one example $(Et_4N)[V_2Fe_2S_4(Me_2dtc)_5]$ [8]. So far a few researches on the V/Fe/S complexes [4,9,10,11] have exhibited their attractive feature to the inorganic and bioinorganic chemists. Holm *et al.* have reported a series of V/Fe/S linear complexes [9], cubane-like clusters [4] and $VFe_4S_6(PEt_3)_4X$ (X = Cl, SR) clusters [10]. Rauchfuss *et al.* have reported several V/Fe/S clusters [11] synthesized by using a divanadium tetrasulfide complexes as starting material. Here we report an assembly system of $VS_4^{3-}/FeCl_2/Et_2dtc^-/PhS^-$ leading to synthesis of a single $[VFe_3S_4]^{3+}$ cubane-like cluster with Et_2dtc^- ligand. Also included in this paper are the structural, spectroscopic and magnetic characterizations for the compound $(Et_4N)[VFe_3S_4(Et_2dtc)_4]$.

EXPERIMENTAL

All manipulations were carried out under dinitrogen atmosphere and Schlenk apparatus was used

* Author to whom correspondence should be addressed.
† Present address: Dept of Chemistry, Zhongshan University, Guangzhou 510275, China.
‡ Naikai University, Tianjin 300071.

throughout the experimental process. The solvents were dried with molecular sieves and degassed prior to use. Reagents $Et_2dtcNa \cdot 3H_2O$ and anhydrous $FeCl_2$, Et_4NCl are commercially available without further purification. Compounds $(NH_4)_3VS_4^9$ and PhSNa [12] were obtained by literature methods.

Synthesis of $(Et_4N)[VFe_3S_4(Et_2dtc)_4]$ (**1**)

A mixture solution of $(NH_4)_3VS_4$ (0.66 g, 2.8 mmol), $FeCl_2$ (1.08 g, 8.5 mmol), $Et_2dtcNa \cdot 3H_2O$ (2.55 g, 11.2 mmol), PhSNa (0.74 g, 5.6 mmol) and Et_4NCl (0.94 g, 5.6 mmol) in 100 ml of CH_3CN was stirred at room temperature for 24 h. After the undissolved material was filtered off, the dark brown–red solution was allowed to stand in the refrigerator for separation of inorganic salt. After filtration the filtrate was again kept in the refrigerator for several days to give black rectangular crystals which were collected, washed with $CH_3CN/(CH_3)_2CO$ (1:1) and dried in vacuo to afford 0.35 g (11.7%, based on V) of product. Anal. calcd for $C_{28}H_{60}Fe_3N_5S_{12}V$: C, 31.43; H, 5.65; Fe, 15.66; N, 6.55; V, 4.76. Found: C, 31.59; H, 5.41; Fe, 14.60; N, 6.54; V, 4.52. IR (KBr, cm^{-1}): 330, 360 (V—S, Fe—S), 991 (C—S), 1143 (C—NR_2) 1492 (C=N). ^1H NMR (DMSO-d_6): δ 1.15 (CH_3, Et_4N), 3.20 (CH_2, Et_4N), 2.07 (CH_3, Et_2dtc), 34.2 (CH_2, Et_2dtcFe), 15.04 (CH_2, Et_2dtcV) ppm. ^{51}V NMR (DMSO-d_6): δ −210 ppm.

Data collection and reduction

A black rectangular crystal of **1** obtained from the reaction solution with approximate dimensions of $0.32 \times 0.18 \times 0.11$ mm was coated with epoxy resin and mounted on a glass fiber. Data collection was performed with Mo-Kα radiation ($\lambda = 0.71073$ Å) on an Enraf–Nonius CAD4 diffractometer equipped with a graphite monochromator at 23 ± 1°C using ω–2θ scan technique. A total of 8952 reflections was collected, of which 8559 were unique. A linear decay, Lorentz-polarization effect and empirical absorption correction based on a series of psi-scans were applied. Intensities of equivalent reflections were averaged.

The crystal and intensity collection are summarized in Table 1.

Structure solution and refinement

The structure was solved by direct methods with MULTAN-83 program. Eight atoms in the cubane skeleton were located from an E-map. The remaining non-hydrogen atoms were located in succeeding difference Fourier syntheses. Though the environments for the four metal atoms in the structure are identical they can be distinguished reasonably of each other by comparison of the M—S bond lengths which were naturally divided into two groups. The two metal

Table 1. Crystallographic data for $(Et_4N)[VFe_3S_4(Et_2NCS_2)_4]$

$C_{28}H_{60}Fe_3N_5S_{12}V$	
formula weight	1070.08
a (Å)	12.599 (2)
b (Å)	19.477 (12)
c (Å)	19.560 (6)
β (°)	100.89 (17)
V (Å^3)	4713.2
Z	4
Space group	$P2_1/n$ (No. 14)
T (°C)	23 ± 1
λ (Å)	0.71073
ρ_{calcd} (g/cm^3)	1.51
μ (cm^{-1})	16.3
R	0.062[a]
R_w	0.059[b]

[a] $R = \Sigma|F_o - F_c|/\Sigma|F_o|$.
[b] $R_w = [\Sigma_w(F_o - F_c)^2/\Sigma_w F_o^2]^{1/2}$.

atoms with shorter M—S distances were recognized to be Fe, while the other two with longer M—S bonds were treated as disorder in terms of M = 0.5V + 0.5Fe [13]. Hydrogen atoms were located and added to the structure factor calculations but their positions were not refined. The structure was refined in full-matrix least-squares procedure using anisotropic thermal parameters for all the non-hydrogen atoms. The function minimized was $\Sigma w(|F_o| - |F_c|)^2$ and the weight w is defined as $4F_o^2/[\sigma(F_o^2)]^2$. Atomic scattering factors were taken from Cromer and Waker [14], the anomalous dispersion effects were included in F_o [15]. The final cycle of refinement included 442 variable parameters for 3392 reflections with $I > 3.0\sigma(I)$ and converged to 0.18σ with unweighted and weighted agreement factors of

$$R_1 = \Sigma|F_o - F_c|/\Sigma|F_o| = 0.062$$

and $$R_2 = [\Sigma w(F_o - F_c)^2/\Sigma w F_o^2]^{1/2} = 0.059$$

The standard deviation of an observation of unit weight was 1.32. The highest and the minimum residual peaks in the final difference Fourier map had a height of 0.74 e/Å^3 and −0.19 e/Å^3, respectively. All calculations were performed on a COMPAQ PL4/50 computer using MolEN/PC program [16].

Other physical measurements

The IR spectrum was recorded on a Bio-Rad FTS-40 Model spectrophotometer. The ^1H and ^{51}V NMR spectra were recorded on a Bruker-Am 500 spectrometer with TMS and $VOCl_3$ as standards, respectively. The Mössbauer spectrum was measured at liquid-nitrogen and room temperature with a constant-acceleration spectrometer using 50 mCi ^{57}Co in a Pd matrix held at 21 ± 1° as the source. Parameters were calibrated with metallic iron at room tempera-

ture. The mass spectroscopic measurement was performed on a Finnigan MAT-8230 GL/MS/DS mass spectrometer in FAB mode at a resolution of 1000. FAB mode: target gas of Ar with pressure of 1 Pa, discharge voltage 8 KV, discharge current 2 mA, m-nitrobenzylalcohol (NBA) matrix. The variable temperature susceptibility was measured on a Model CF-1 superconducting extraction sample magnetometer with the crystalline sample kept in a capsule at 1.5 ~ 300 K. Elemental analyses were carried out by the Analytical Chemistry Group of this Institute.

RESULTS AND DISCUSSION

Synthesis

The self-assembly systems containing tetrathiometallate (metal M = W, Mo [1a,2,5,6,17] V [2b,4,7,9,18], Re [19] Nb [4d,20]) and metal halide (metal M′ = Fe, Ag, Cu) have been extensively used to synthesize a series of heterometal–sulfur cluster compounds, among which the $[M_nM'_{4-n}S_4]$ ($n = 1, 2$) cubane-like clusters are always expected if the tetrathiometallate is reduced in the reaction process. Holm and coworkers have prepared single and double $[VFe_3S_4]^{2+,3+}$ cubane-like clusters by using $VS_4^{3-}/FeCl_2/RS^-$ assembly system. In previous work, we have reported the assembly systems of $VS_4^{3-}/FeCl_2/Me_2dtc^-$ and isolated $(Et_4N)[V_2Fe_2S_4(Me_2dtc)_5]$ cluster compound (**2**) [8]. Interestingly, the R group in the R_2dtc^- reveals an obvious effect on the products formed in the reaction system. Diethyldithiocarbamate leads to the $[VFe_3S_4]^{3+}$ cubane-like cluster, while Me_2dtc^- leads to the $V_2Fe_2S_4$ cubane-like cluster under similar assembly system, in which PhS^- is also a part. Also, in the case of Bz_2dtc^-, a mononuclear complex $Fe(Bz_2dtc)_3$ becomes the only separable product. It appears that the steric effect of bulky group hinders the formation of polynuclear metal complex.

It is also noteworthy that the present assembly system of mixed ligands, R_2dtc^- and PhS^-, only results in the generation of the cluster which contains no PhS^- ligand. This indicates that the bidentate R_2dtc^- is superior to the monodentate thiolate in competitive coordinating to vanadium and iron ions. However, PhS^- in the assembly system should not be ignored since its participation is useful in the reduction of VS_4^{3-} leading to the formation of the VFe_3S_4 cubane-like cluster. A control experiment, in which PhS^- is not used, has been carried out resulting in the separation of no VFe_3S_4 cluster. Similar results have also been observed in preparing other $[VFe_3S_4(R_2dtc)_4]^-$ clusters ($R_2 = OC_4H_8$, C_5H_{10}).

Structure

The crystal structure of cluster **1** consists of four discrete cluster anions and four Et_4N^+ cations which are well separated from the respective anions. An ORTEP drawing of the cluster anion is depicted in Fig. 1, and the selected interatomic bond distances and angles are shown in Tables 2 and 3, respectively.

The anion contains a VFe_3S_4 distorted cuboidal core, in which all the metal/sulfur rhombic units such as Fe_2S_2 and M_2S_2 are nonplanar except for the Fe(2)M(2)S(1)S(3) unit whose atoms have the largest deviation of 0.003 Å from the least-square plane. Each metal atom is chelated by a Et_2dtc^- ligand and coordinated by three inorganic S atoms to form a distorted trigonal bipyramidal geometry. The Fe—S_{dtc} bond distance of 2.423(21) Å (av.) is intermediate between those of $MoFe_3S_4(Et_2dtc)_5$ (2.299 Å) [5a] and $[MoFe_3S_4(Et_2dtc)_5]^-$ (2.524 Å) [5a] implying that the Fe mean oxidation state is intermediate between +3 for the former and +2.67 for the latter. A similar comparison with complex **2** which contains Fe^{III} atoms and Fe—S_{dtc} bonds of 2.321(18) Å (mean) shows also that compound **1** has three Fe atoms with the mean oxidation state to be not higher than or near to +3. Mean Fe—S_{core} bond distance (2.276(16) Å) of **1** is longer than those of $MoFe_3S_4(R_2dtc)_5$ (2.223(16) Å) [5a] and **2** (2.240(3) Å) [8], supporting also the evaluation of the above oxidation state for Fe. The metal–metal distances in the VFe_3S_4 core range from 2.795(2) to 2.994(3) Å showing obvious intermetallic interactions. The M(1)—M(2) distance of 2.834(3) Å which represents the V—Fe distance is comparable to the V—Fe distance [av. 2.780(6) Å] [8] in **2**, while the Fe(1)—Fe(2) distance of 2.795(2) Å is also comparable to those of **2** [2.681(2) Å] [8] and $MoFe_3S_4(R_2dtc)_5$ [av. 2.706(18) Å] [5a]. However, owing to the disorder of the M sites, the structural discussion could not be presented in further detail.

Infrared spectrum

In the low frequency region, the absorption in 330–360 cm^{-1} are assigned to Fe—S_{dtc} and V—S_{dtc} vibrations [21]. In the 400–500 cm^{-1} region where the M–μ_3–S vibrations are expected [22], several weak and wide absorptions with obscurity appear showing a distinguishing characteristic of the VFe_3S_4 cuboidal core just like the IR spectrum of $MoFe_3S_4(R_2dtc)_5$ in the same area [5b].

NMR spectrum

^1H and ^{51}V NMR spectra are depicted in Fig. 2. There are two types of Et_2dtc groups in the complex, Et_2dtcFe and Et_2dtcV, corresponding to the two sets of signals at 34.2 and 15.0 ppm, respectively, with the intensity ratio of about 3:1 in the ^1H spectrum. In comparison with Et_2dtcNa ($\delta_{\alpha\text{-}H}$: 3.99 ppm), the proton chemical shifts of the —NCH_2— in ligands move obviously to downfield indicating the paramagneticity of the cluster. The ^1H NMR shift of Et_2dtc associated to the Fe site is consistent with that in compounds

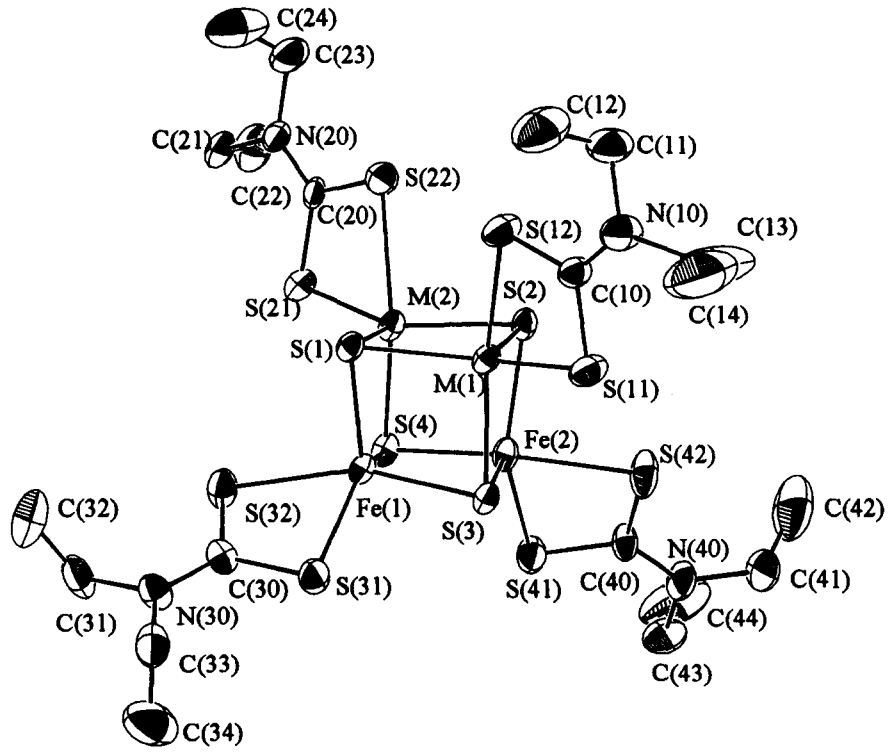

Fig. 1. ORTEP diagrams showing 50% probability ellipsoids for the anion $[VFe_3S_4(Et_2dtc)_4]^-$ with numbering scheme.

Table 2. Selected bond lengths (Å) for the $[VFe_3S_4(Et_2dtc)_4]^-$ anion

Fe(1)—Fe(2)	2.795(2)	M(1)—M(2)	2.834(3)
Fe(1)—M(1)	2.988(3)	Fe(2)—M(1)	2.805(3)
Fe(1)—M(2)	2.814(2)	Fe(2)—M(2)	2.994(3)
	mean (Fe—M)	2.90(5)[a]	
Fe(1)—S(1)	2.272(4)	M(1)—S(1)	2.335(3)
Fe(1)—S(3)	2.323(4)	M(1)—S(2)	2.280(3)
Fe(1)—S(4)	2.255(3)	M(1)—S(3)	2.355(4)
Fe(2)—S(2)	2.298(4)	M(2)—S(1)	2.272(3)
Fe(2)—S(3)	2.213(3)	M(2)—S(2)	2.323(4)
Fe(2)—S(4)	2.296(4)	M(2)—S(4)	2.369(4)
mean	2.276(16)[a]	mean	2.321(16)[a]
Fe(1)—S(31)	2.394(4)	M(1)—S(11)	2.413(4)
Fe(1)—S(32)	2.473(5)	M(1)—S(12)	2.513(4)
Fe(2)—S(41)	2.385(5)	M(2)—S(21)	2.398(5)
Fe(2)—S(42)	2.441(5)	M(2)—S(22)	2.586(4)
mean	2.423(21)[a]	mean	2.478(44)[a]
S(11)—C(10)	1.72(1)	S(31)—C(30)	1.72(1)
S(12)—C(10)	1.67(1)	S(32)—C(30)	1.69(1)
S(21)—C(20)	1.71(1)	S(41)—C(40)	1.68(1)
S(22)—C(20)	1.70(1)	S(42)—C(40)	1.71(1)
	mean	1.70(1)[a]	
C(10)—N(10)	1.34(2)	C(30)—N(30)	1.33(1)
C(20)—N(20)	1.31(2)	C(40)—N(40)	1.33(2)
	mean	1.33(1)[a]	

Numbers in parentheses are estimated standard deviations in the least significant digits.

[a]Standard deviation of the mean value is estimated from $\sigma = [\Sigma_{i=1}^{N} (Xi - \bar{X})^2/N(N-1)]^{1/2}$.

with $Fe^{III}(Et_2dtc)$ group, such as $Fe_4S_4(Et_2dtc)_4$ ($\delta_{\alpha\text{-H}}$: 33.0 ppm, $\delta_{\beta\text{-H}}$: 2.2 ppm) [5a] and $MoFe_3S_4(Et_2dtc)_5$ ($\delta_{\alpha\text{-H}}$: 32.8 ppm) [5a]. For the latter, its Fe^{III} spin states of $S = 1/2$ have been determined [23], implying that the Fe atoms of **1** may have low spin d^5 ground state being used to the treatment of magnetic data (*vide infra*). The general features of ^{51}V NMR shift depend strongly upon the oxidation state and coordination environment (ligands electronegativity and coordination number, etc.) of the vanadium [24,25]. Compared to VS_4^{3-} ($\delta\ ^{51}V$: −1388 ppm) [26] the five-coordinate vanadium nucleus in complex **1** has a lower oxidation state and larger shielding effect, giving rise to the ^{51}V absorption peak upfield at −210 ppm. Although both **1** and **2** containing R_2dtc and sulfide ligating environment have closely related structures and have near ^{51}V NMR shifts (−391 ppm [8] for **2**), it is difficult to make a reasonable comparison because of the difference between V nuclei of the two complexes.

Mössbauer spectrum

Mössbauer parameters obtained by least-squares fitting with the experimental absorption spectrum are shown in Table 4 together with the data of other related clusters containing metal atoms in the same coordination environment. The solid Mössbauer spectrum of cluster **1** shown in Fig. 3 consists of two

Table 3. Selected bond angles (°) for the $[VFe_3S_4(Et_2dtc)_4]^-$ anion

S(1)—M(1)—S(2)	103.1(1)	S(1)—Fe(1)—S(3)	98.1(1)
S(1)—M(1)—S(3)	95.5(1)	S(1)—Fe(1)—S(4)	105.6(1)
S(2)—M(1)—S(3)	101.8(1)	S(3)—Fe(1)—S(4)	101.9(1)
S(1)—M(1)—S(11)	137.7(1)	S(1)—Fe(1)—S(31)	115.2(1)
S(1)—M(1)—S(12)	91.7(1)	S(1)—Fe(1)—S(32)	96.6(1)
S(2)—M(1)—S(11)	117.2(1)	S(3)—Fe(1)—S(31)	87.1(1)
S(2)—M(1)—S(12)	98.4(1)	S(3)—Fe(1)—S(32)	158.1(1)
S(3)—M(1)—S(11)	88.7(1)	S(4)—Fe(1)—S(31)	136.1(1)
S(3)—M(1)—S(12)	156.4(1)	S(4)—Fe(1)—S(32)	89.6(1)
S(11)—M(1)—S(12)	71.1(1)	S(31)—Fe(1)—S(32)	71.9(1)
S(1)—M(2)—S(2)	104.0(1)	S(2)—Fe(2)—S(3)	105.7(1)
S(1)—M(2)—S(4)	101.9(1)	S(2)—Fe(2)—S(4)	97.3(1)
S(2)—M(2)—S(4)	94.9(1)	S(3)—Fe(2)—S(4)	104.1(1)
S(1)—M(2)—S(21)	118.1(1)	S(2)—Fe(2)—S(41)	137.6(1)
S(1)—M(2)—S(22)	96.5(1)	S(2)—FE(2)—S(42)	89.8(1)
S(2)—M(2)—S(21)	135.8(1)	S(3)—Fe(2)—S(41)	114.1(1)
S(2)—M(2)—S(22)	93.1(1)	S(3)—Fe(2)—S(42)	97.0(1)
S(4)—M(2)—S(21)	89.2(1)	S(4)—Fe(2)—S(41)	86.9(1)
S(4)—M(2)—S(22)	157.5(1)	S(4)—Fe(2)—S(42)	154.9(1)
S(21)—M(2)—S(22)	70.6(1)	S(41)—Fe(2)—S(42)	72.0(1)
M(1)—S(1)—M(2)	75.9(1)	M(1)—S(3)—Fe(1)	79.4(1)
M(1)—S(1)—Fe(1)	80.8(1)	M(1)—S(3)—Fe(2)	75.7(1)
M(2)—S(1)—Fe(1)	76.5(1)	Fe(1)—S(3)—Fe(2)	76.0(1)
M(1)—S(2)—M(2)	76.2(2)	M(2)—S(4)—Fe(1)	74.9(1)
M(1)—S(2)—Fe(2)	75.6(2)	M(2)—S(4)—Fe(2)	79.8(1)
M(2)—S(2)—Fe(2)	81.0(1)	Fe(1)—S(4)—Fe(2)	75.8(1)
S(11)—C(10)—S(12)	115.5(7)	S(31)—C(30)—S(32)	114.1(6)
S(11)—C(10)—N(10)	121(2)	S(31)—C(30)—N(30)	123.9(9)
S(12)—C(10)—N(10)	123(2)	S(32)—C(30)—N(30)	123(1)
S(21)—C(20)—S(22)	115.3(7)	S(41)—C(40)—S(42)	113.1(7)
S(21)—C(20)—N(20)	122.0(9)	S(41)—C(40)—N(40)	125.6(9)
S(22)—C(20)—N(20)	122.7(9)	S(42)—C(40)—N(40)	121(1)

Numbers in parentheses are estimated standard deviations in the least significant digits.

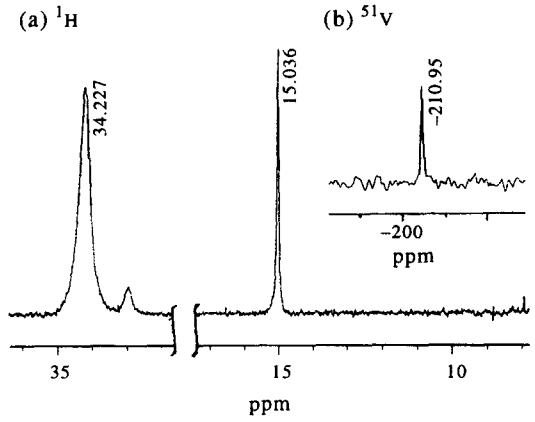

Fig. 2. (a) ^{1}H NMR spectrum of $(Et_4N)[VFe_3S_4(Et_2dtc)_4]$ in DMSO-d_6 solution at room temperature with the part of Et_4N^+ omitted. (b) ^{51}V NMR spectrum of $(Et_4N)[VFe_3S_4(Et_2dtc)_4]$ in DMSO-d_6 solution at room temperature with $VOCl_3$ as standard.

overlapping symmetric quadrupole doublets with isomer shifts (IS) of 0.46(2) and 0.50(2) mm/s, quadrupole splittings (QS) of 0.99(2) and 0.62(2) mm/s, and absorption intensity ratio of 2:1 indicating that two sets of Fe sites have a small inequivalence which happens to be consistent with the disordered treatment of the Fe/V atoms in the structure solution.

In comparison with compound **2** which has 5-coordinate Fe^{III} atoms in a $V_2Fe_2S_4$ cuboidal skeleton, **1** has a somewhat larger IS value indicating that it has a Fe mean oxidation state lower than Fe^{III}. Meanwhile, the IS values for **1** are intermediate between those of $[MoFe_3S_4(Et_2dtc)_5]^-$ and $[MoFe_3S_4(Et_2dtc)_5]$ [5a], in which the Fe mean oxidation states range from 2.67+ to 3+, respectively. According to empirical relationship $IS = 1.902 - 0.506X$, which we have suggested [8] to evaluate the Fe (mean) oxidation state (X) in 5-coordinate FeS_5 sites containing R_2dtc^- ligands (s), the Fe mean oxidation state in cluster **1** is deduced as $X = 2.82$. Similar formula for the 4-coordinate Fe in tetrahedral FeS_4 sites has been presented by Holm and co-workers [4d,10b,28].

Mass spectrum

Fast atom bombardment mass spectrometry (FAB-MS) was used to obtain the data of main fragments containing metal ion and their relative abundances

Table 4. Isomer shifts (IS, mm/s) and quadrupole splittings (QS, mm/s) of 5-coordinate Fe sites at 77 K for $[VFe_3S_4(Et_2dtc)_4]^-$ and related compounds

Compound	Oxidation state	IS[b]	QS	Ref.
$[VFe_3S_4(Et_2dtc)_4]^-$	$< +3(2.82)$[a]	0.46, 0.50	0.99, 0.62	this work
$[V_2Fe_2S_4(Me_2dtc)_5]^-$	+3(2.93)	0.42	0.23	[8]
$MoFe_3S_4(Et_2dtc)_5$	+3(3.03)	0.37	1.36	[5a]
$Fe_4S_4(Et_2dtc)_4$	+3(2.95)	0.41	1.42	[5a]
$[MoFe_3S_4(Et_2dtc)_5]^-$	+2.67(2.69)	0.54	1.18	[5a]
$[Fe_4S_4(PhS)_2(Et_2dtc)_2]^{2-}$	+2.5(2.49)	0.64	1.84	[27]

[a] The data in the parentheses are deduced according to the eq. IS = $1.902 - 0.506X$ [8].
[b] Relative to Fe metal at room temperature.

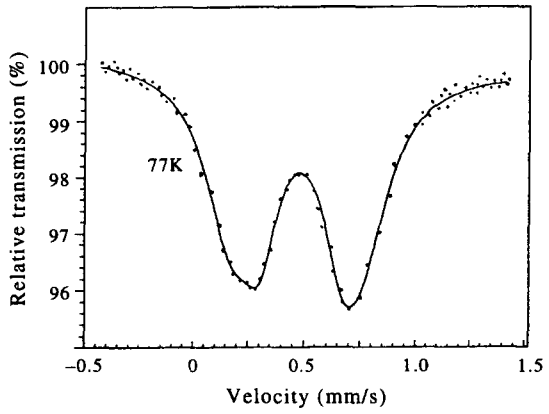

Fig. 3. Mössbauer spectrum of $(Et_4N)[VFe_3S_4(Et_2dtc)_4]$ at liquid-nitrogen temperature. Solid line represents the least-squares fits for the experimental data.

Table 5. The main metal-containing fragment ions and their relative abundance in the positive ion FAB mass spectrum of cluster the $(Et_4N)[VFe_3S_4(Et_2dtc)_4]$ using the matrix NBA

Ion	*m/z*	Relative abundance
$\{(Et_4N)[VFe_3S_4L_4]\}^+$[a]	1069	unobserved
$[VFe_3S_4L_4]^+$	939	unobserved
$[VFe_3S_4L(NBA)_3]^+$[b]	951	0.33
$[VFe_3S_4L(NBA)]^+$	647	0.73
$[VFe_3S_3L(NBA)]^+$	615	0.68
$[Fe_3S_4L_3]^+$	740	0.26
$[Fe_3S_4L_2]^+$	592	0.24
$[Fe_3S_3L_3]^+$	708	0.13
$[Fe_2S_4L_2]^+$	536	0.15
$[Fe_2S_3L_2]^+$	504	0.21
$[Fe_2S_2L_2]^+$	472	0.21
$[Fe_2S_2L]^+$	324	0.74
$[Fe_2SL_2]^+$	440	0.17
$[Fe_2L_2]^+$	408	0.41
$[FeL_2]^+$	352	9.39
Et_4N^+	130	100

[a] $L = Et_2NCS_2^-$.
[b] NBA = m-$NO_2C_6H_4CH_2O^-$.

referring to Et_4N^+ (m/z 130) for the cubane-type cluster $(Et_4N)[VFe_3S_4L_4]$ ($L = Et_2NCS_2^-$) as shown in Table 5. The breakdown of the cluster skeleton is considered as the major cleavage process indicated by the occurrence of fragments ions $[Fe_3S_4L_3]^+$ (m/z 740), $[Fe_3S_3L_3]^+$ (m/z 708), $[Fe_3S_4L_2]^+$ (m/z 592), $[Fe_2S_4L_2]^+$ (m/z 536), $[Fe_2S_3L_2]^+$ (m/z 504), $[Fe_2S_2L_2]^+$ (m/z 472), $[Fe_2S_2L]^+$ (m/z 324), $[Fe_2SL_2]^+$ (m/z 440), $[Fe_2L_2]^+$ (m/z 408) and FeL_2^+ (m/z 352), of which the last one is the metal fragment of the highest relative abundance. Some ion spices retaining VFe_3S_4 skeleton, such as $[VFe_3S_4L(NBA)_3]^+$ (m/z 951) and $[VFe_3S_4L(NBA)]^+$ (m/z 647) have been observed showing a process of the substitution [29] of $Et_2NCS_2^-$ by the matrix molecules NBA and subsequent loss of m-nitrobenzylalcoholate.

$$\underset{(m/z\,939)}{[VFe_3S_4L_4]^+} \xrightarrow[-3L]{+3NBA} \underset{(m/z\,951)}{[VFe_3S_4L(NBA)_3]^+} \xrightarrow[-2NBA]{} \underset{(m/z\,647)}{[VFe_3S_4L(NBA)]^+}$$

The peak of the cluster ion $[VFe_3S_4L_4]^+$ (m/z 939) was not observed showing its low stability in the positive FAB-MS. However the peak of cluster anion $[VFe_3S_4L_4]^-$ has been obtained in the negative FAB mode.

Magnetic properties

Magnetic susceptibility data for the solid sample of **1** were collected in the temperature range 1.5 ~ 300 K, as shown in Fig. 4. With the rising of temperature, the magnetic moments of the cluster rise quickly in the range 1.5–24 K and then rise slowly beyond 24 K, implying that a weak antiferromagnetic spin-exchange interaction is operating in the molecule. In order to understand quantitatively the magnitudes of spin-exchange interaction between the magnetic centers,

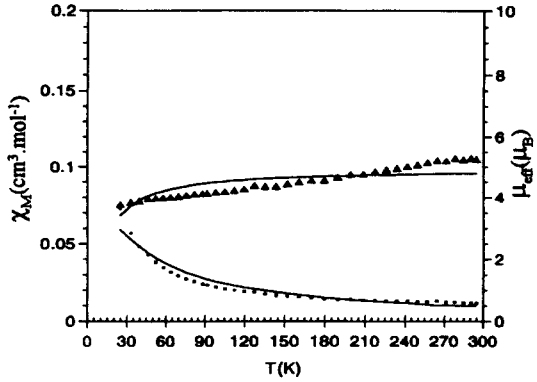

Fig. 4. Experimental molar susceptibility (χ_M ■) and effect magnetic moment (μ_{eff} ▲) of temperature dependence for $(Et_4N)[VFe_3S_4(Et_2dtc)_4]$. The solid line (–) represents the respective calculated values.

the spin system in $[VFe_3S_4]$ cubane-like cluster can be modeled as the following scheme.

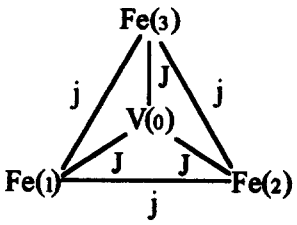

Thus the spin Hamiltonian appropriate for the magnetic exchange interaction in the VFe_3 coupling system is presented as the following equation.

$$\hat{H} = -2j(\hat{S}_1\hat{S}_2 + \hat{S}_1\hat{S}_3 + \hat{S}_2\hat{S}_3) - 2J(\hat{S}_1\hat{S}_0 + \hat{S}_2\hat{S}_0 + \hat{S}_3\hat{S}_0)$$

where S_j is the spin angular momentum operator for the magnetic centers $M(i)$, j and J are exchange coupling constants between Fe atoms and between V and Fe atoms, respectively, characterizing the exchange interaction. On the basis of $3Fe^{III}+V^{II}$ oxidation states, which may be a more reasonable choice than that of $2Fe^{III}+Fe^{II}+V^{III}$ according to above-mentioned discussion, three Fe^{III} sites are supposed to be in a low spin state of $S_1 = S_2 = S_3 = 1/2$ and the V^{II} site in a high spin state of $S_0 = 3/2$. By applying the Van Vleck Equation [30], the following molar susceptibility expression for the coupling system $VFe_3(S_1 = S_2 = S_3 = 1/2,\ S_0 = 3/2)$ can be easily obtained

$$\chi_M = \frac{2Ng^2\beta^2}{KT}\left|\frac{A}{B}\right|$$

where

$$A = 14 + 5\exp(-6J/KT) + \exp(-10J/KT) + 10\exp((-3J-3j)/KT) + 2\exp((-7J-3j)/KT),$$

$$B = 7 + 5\exp(-6J/KT) + 3\exp(-10J/KT) + \exp(-12J/KT) + 10\exp((-3J-3j)/KT) + 6\exp((-7J-3j)/KT)$$

and each symbol has its usual meaning.

The experimental data and the theoretical fitting results of the molar magnetic susceptibility (χ_M) versus temperature (T) ranging from 24 to 300 K are depicted in Fig. 4, giving $J = -4.12\ cm^{-1}$, $j = -5.82\ cm^{-1}$, $g = 2.02$ and $F = 4.9 \times 10^{-4}$ which is defined as $\Sigma[(\chi_M)_{obs} - (\chi_M)_{calc}]^2/(\chi_M)_{obs}$. The results ($J$ or $j < 0$ and $|J|$ or $|j|$ is small) indicate the existence of a weak antiferromagnetic spin interactions between V^{II} and Fe^{III} and between Fe^{III} atoms. The data below 24 K were not treated because the effect of zero-field splitting and intermolecular interactions become significant.

Acknowledgements—We are grateful for the financial assistance from the Climbing Program-National Key Project for Fundamental Research in China and the National Science Foundation of China. Thank are also due to the Center of Analysis and Measurement of Zhongguancun, Beijing for measurement of the variable temperature magnetic susceptibility.

Supplementary material available—Tables of crystallographic data, atomic coordinates, bond lengths and angles and anisotropic thermal parameters (7 pages).

REFERENCES

1. (a) Holm, R. H., *Chem. Soc. Rev.*, 1981, **10,** 455; (b) Burgess, B. K., *Chem. Rev.*, 1990, **90,** 1377.
2. (a) Holm, R. H. and Simhon, E. D., In *Molybdenum Enzymes*; T. D. Spiro, Ed.; Wiley-Interscience, New York (1985), chapter 2 and refs therein; (b) Holm, R. H., *Adv. Inorg. Chem.*, 1992, **38,** 1 and relative refs therein; (c) Coucouvanis, D., *Acc. Chem. Res.*, 1991, **24,** 1 and refs therein.
3. (a) Kim, J. and Rees, D. C., *Nature*, 1992, **360,** 553; (b) Chan, M. K., Kim, J. and Rees, D. C., *Science*, 1993, **260,** 792; (c) Kim, J., Woo, D. and Rees, D. C., *Biochemistry*, 1993, **32,** 7104.
4. (a) Kovacs, J. A. and Holm, R. H., *J. Am. Chem. Soc.*, 1986, **108,** 340; (b) Kovacs, J. A. and Holm, R. H., *Inorg. Chem.*, 1987, **26,** 711; (c) Kovacs, J. A. and Holm, R. A., *Inorg. Chem.*, 1987, **26,** 702; (d) Cen, W., Lee, S. C., Li, J., MacDonnell, F. M. and Holm, R. H., *J. Am. Chem. Soc.*, 1993, **115,** 9515.
5. (a) Liu, Q., Huang, L., Liu, H., Lei, X., Wu, D., Kang, B. and Lu, J., *Inorg. Chem.*, 1990, **29,** 4131 and refs therein; (b) Liu, Q., Lei, X., Huang, L., Chen, W., Zhao, K., Chen, D., Liu, H. and Lu, J., *Sci. Sin.*, 1990, **B33,** 1446; (c) Liu, Q., Huang, L., Lei, X., Wang, F., Chen, D. and Lu, J., *Sci. Sin.*, 1991, **B34,** 1036.
6. (a) Lei, X., Huang, Z., Liu, Q., Hong, M. and Liu, H., *Inorg. Chem.*, 1989, **28,** 4302; (b) Lei, X., Huang, Z., Liu, Q., Hong, M. and Liu, H., *Inorg. Chim. Acta*, 1989, **164,** 119; (c) Liu, H., Cao, R.,

Lei, X., Huang, Z., Hong, M. and Kang, B., *J. Chem. Soc., Dalton Trans.*, 1990, 1023.

7. (a) Yang, Y., Liu, Q., Huang, L., Kang, B. and Lu, J., *J. Chem. Soc. Chem. Commun.*, 1992, 1512; (b) Yang, Y. and Liu, Q., *Acta Crystallogr.*, 1993, **C49,** 1623; (c) Yang, Y., Liu, Q., Huang, L., Wu, D., Kang, B. and Lu, J., *Inorg. Chem.*, 1993, **32,** 5431; (d) Liu, Q., Yang, Y., Huang, L., Wu, D., Kang, B., Chen, C., Deng, Y. and Lu, J., *Inorg. Chem.*, 1995, **34,** 1884; (e) Yang, Y., Liu, Q., Kang, B. and Lu, J. *Science in China*, 1995, **B38,** 264.
8. Deng, Y., Liu, Q., Yang, Y., Wang, Y., Cai, Y., Wu, D., Chen, C., Liao, D., Kang, B. and Lu, J., *Inorg. Chem.*, 1997, **36,** 214.
9. Do, Y., Simhon, E. D. and Holm, R. H., *Inorg. Chem.*, 1985, **24,** 4635.
10. (a) Nordlander, E., Lee, S. C., Cen, W., Wu, Z. Y., Natoli, C. R., Cicco, A. D., Filipponi, A., Hedman, B., Hodgson, K. O. and Holm, R. H., *J. Am. Chem. Soc.*, 1993, **115,** 5549; (b) Cen, W., MacDonnell, F. M., Scott, M. J. and Holm, R. H., *Inorg. Chem.*, 1994, **33,** 5809.
11. (a) Rauchfuss, T. B., Weatherill, T. D., Wilson, S. R. and Zebrowski, J. P., *J. Am. Chem. Soc.*, 1983, **105,** 6508; (b) Bolinger, C. M., Weatherill, T. D., Rauchfuss, T. B., Rheingold, A. L., Day, C. S. and Wilson, S. R., *Inorg. Chem.*, 1986, **25,** 634.
12. Hagen, K. S., Reynolds, J. G. and Holm, R. H., *J. Am. Chem. Soc.*, 1981, **103,** 4054.
13. (a) There are several choices for the disordered treatment of the metal atoms in the solution of the structure: M(1) = M(2) = M(3) = M(4) = 1/4V+3/4Fe; M(1) = M(2) = 1/2V+1/2Fe (M(1) and M(2) contain longer M—S bonds) and M(1) = M(2) = 1/2 V+1/2 Fe (M(1) and M(2) contain shorter M—S bonds). Since bond distance of V^{III}—S_{dtc} is longer than that of Fe^{III}—S_{dtc} in the same coordination environment, such as $V(Bu_2dtc)_3$ [13b] (2.43 Å), $V(Et_2dtc)_3$ [13c] (2.434(3) Å), and $Fe(Et_2dtc)_3$ [13d] (2.358(2) Å), V^{II}—S_{dtc} bond should still be longer. Besides, spectroscopic and magnetic parameters also tentatively support the metal oxidation states of V^{II}+3Fe^{III}, therefore, the disordered treatment of 1/2V+1/2Fe for the two metal atoms with longer M—S bonds seems to be the best choice; (b) Porter, L. C., Novick, S. G. and Murray, H. H., *J. Coord. Chem.*, 1994, **31,** 47; (c) Zhu, H., Deng, Y., Huang, X., Chen, C., and Liu, Q., *Acta Crystallogr.*, 1997, **C53,** in press. (d) Leipoldt, J. G. and Coppens, P., *Inorg. Chem.*, 1973, **12,** 2269.
14. Cromer, D. T. and Waber, J. T., *International Tables for X-Ray Crystallography*, Vol. IV, Table 2.2B and Table 2.3.1. J. A. Ibers and W. C. Hamilton, Eds., The Kynoch Press, Birmingham, England (1974).
15. Ibers, J. A. and Hamilton, W. C., *Acta Crystallogr.*, 1964, **15,** 781.
16. MolEN, *An Interactive Structure Solution Procedure*. Enraf-Nonius, Delft, The Netherlands (1990).
17. Jeannin, Y., Sécheresse, F., Bernès, S. and Robert, F., *Inorg. Chem. Acta*, 1992, **198–200**, 493 and refs therein.
18. (a) Müller, A., Schimanski, J. and Bögge, H., *Z. Anorg. Allg. Chem.*, 1987, **554,** 107; (b) Scattergood, C. D., Bonney, P. G., Slater, J. M., Garner, C. D. and Clegg, W., *J. Chem. Soc., Chem. Commun.*, 1987, 1749.
19. (a) Ciurli, S., Carney, M. J., Holm, R. H. and Papaefthymiou, G. C., *Inorg. Chem.*, 1989, **28,** 2696; (b) Ciurli, S., Carrié, M. and Holm, R. H., *Inorg. Chem.*, 1990, **29,** 3493; (c) Ciurli, S. and Holm, R. H., *Inorg. Chem.*, 1991, **30,** 743; (d) Müller, A., Krickemeyer, E., Hildebrand, A., Bögge, H., Schneider, K. and Lemke, M., *J. Chem. Soc., Chem. Commun.*, 1991, 1685 and refs therein.
20. Lee, S. C. and Holm, R. H., *J. Am. Chem. Soc.*, 1990, **112,** 9654.
21. Bradley, D. C. and Gitlitz, M. H., *J. Chem. Soc.*, 1969(A), 1152.
22. Müller, A., Jaegermann, W. and Helmann, W., *J. Mol. Struc.*, 1983, **100,** 559.
23. Liu, Q., Deng, Y., Chen, C., Liao, D. and Cui, J., *Jiegou Huaxue*, 1996, **15,** 408.
24. (a) Sendlinger, S. C., Nicholson, J. R., Lobkovsky, E. B., Huffman, J. C., Rehder, L. and Christou, G., *Inorg. Chem.*, 1993, **32,** 204.
25. (a) Howarth, O. W., *Progress in NMR Spectroscopy*, 1990, **22,** 453; (b) Harrison, T. and Howarth, O. W., *J. Chem. Soc., Dalton Trans.*, 1986, 1405.
26. Zhang, Y. and Holm, R. H., *Inorg. Chem.*, 1988, **27,** 3875.
27. Kanatzidis, M. G., Coucouvanis, D., Simopoulos, A., Kostikas, A. and Papaefthymiou, V., *J. Am. Chem. Soc.*, 1985, **107,** 4925.
28. Christou, G., Mascharak, P. K., Armstrong, W. H., Papaefthymiou, F. C., Frankel, R. B. and Holm, R. H., *J. Am. Chem. Soc.*, 1982, **104,** 2820.
29. Lee, W. L., Gage, D. A., Huang, H., Chang, C. K., Kanatzidis, M. G. and Allison, J., *J. Am. Chem. Soc.*, 1992, **114,** 7132.
30. Van Vleck, J. H., *Electric and Magnetic Susceptibilities*. Oxford Univ. Press, London (1992).